Hygric and Thermal Insulation Properties of Building Materials Based on Bamboo Fibers

Dang Mao Nguyen[1(✉)], Anne-Cécile Grillet[1], Thi My Hanh Diep[2], Thi Vi Vi Do[3], Chi Nhan Ha Thuc[3], and Monika Woloszyn[1]

[1] LOCIE, UMR Université de Savoie Mont Blanc - CNRS, 73000 Chambéry, France
{mao.nguyen-dang, anne-cecile.grillet, Monika.Woloszyn}@univ-savoie.fr
[2] Research Center Scientific for Conservation of Natural Resources, University of Sciences, Vietnam National University Ho Chi Minh City (VNU), Ho Chi Minh City, Vietnam
mhg286@gmail.com
[3] Faculty of Material Science, University of Science, Vietnam National University Ho Chi Minh City (VNU), Ho Chi Minh City, Vietnam
dtvvi@hcmuns.edu.vn, htcnhan@hcmus.edu.vn

Abstract. This study focuses on manufacturing bio-insulation fiberboards from bamboo fibers and bone glue, modified with sodium lignosulfonate. The microstructure of these boards is investigated by mercury intrusion porosimetry. The porosity and average pore size of boards are decreased; however, the specific pore surface is increased with the presence of bio-glues in boards. The hygric properties are examined through kinetics of water vapor sorption at equilibrium states. The thermal conductivity and bending properties are also studied. The thermal conductivity is dependent on relative humidity levels and moisture content of the fiberboards. The bending property is increased with 30% (w/w) of mixture glue between bone and sodium lignosulfonate in boards.

Keywords: Thermal conductivity · Bamboo fiberboards · Kinetics of vapor sorption · Microstructure · Bio-insulation material

1 Introduction

In a context of reducing energy consumption for future buildings, this research deals with bio-insulation materials incorporating between bamboo fibers and biological protein/lignin binders. The materials are applied inside buildings in order to control humidity when environmental condition changes. Especially, they can improve the moisture buffering capacity due to their porous structure and high moisture absorbing capacity inducing by protein and protein/sodium lignosulfonate mixture glues. The protein based bone glue and mixture between bone and sodium lignosulfonate compound are currently interested in as effective binders for wood-based products industry.

H. Tran-Nguyen et al. (eds.), *Proceedings of the 4th Congrès International de Géotechnique - Ouvrages -Structures*, Lecture Notes in Civil Engineering 8,
DOI 10.1007/978-981-10-6713-6_50

On the other hand, in the past, the most popular board materials such as fiberboard, particleboard, medium-density fiberboard (MDF) and high-density fiberboard (HDF) used phenol–formaldehyde (PF), urea–formaldehyde (UF), urea–melamine–formaldehyde (UMF) as effective glues for providing excellent mechanical properties and high-water resistances under various conditions. However, these products release formaldehyde into the air causing a great problem for the environment and for humans. Indeed, exposure to air born formaldehyde can result in health effects such as skin irritation, watery eyes, coughing and nausea. Furthermore, prolonged exposure to formaldehyde can cause certain types of cancer such as nasopharyngeal cancer (Hauptmann et al. 2004; Michael et al. 2009). Consequently, there is a strong need for the development of environment-friendly fiberboards. For example, research works are conducted on fiberboards based on natural fibers, agricultural waste combined with bio-adhesives such as vegetable oil, chitin, lignin and protein because they are renewable, biodegradable and highly hygroscopic products with low environmental impact. In order to produce new glues, the modification of different proteins has been investigated by researchers. Lignin is often used to modify various proteins including proteins based on wheat gluten (Duval et al. 2013; Kaewtatip et al. 2010; Khosravi et al. 2011; Kunanopparat et al. 2009; Kunanopparat et al. 2012), soybean (Huang and Chen 2003; Zhigang et al. 2013) and protein from maize (Cong et al. 2013). Lignin has a good compatibility with mixtures of proteins leading to an increase in mechanical properties and water resistance. In fact, the lignin has effective interactions with many kinds of proteins and natural fibers via hydrogen or covalent bonds.

The natural fibers based building insulation materials are well known of porous structure, the microstructure and hygrothermal performance link to their porous structure. The porous structure of materials was investigated through many techniques; the most widely used methods are focused on nitrogen sorption isotherms, mercury intrusion porosimetry (MIP) and scanning electron microscopy (SEM). In particular, porous structure and water vapor sorption of hemp-based materials were examined via MIP technique and water vapor sorption with BJH mode (Collet et al. 2008). Moreover, the total pore surface area, porosity and micropores structure of waste wood based cement-bonded particleboards were studied by MIP method and the pores size distribution was classified into three zones of pores (capillary, mesopores and air) (Wang et al. 2017). The same MIP tested method and classifications were also applied for microstructure characterization of waste wood based noise and thermal insulating cement-bonded particleboards (Wang et al. 2016).

Moreover, the hygrothermal properties of insulation materials are evaluated by their thermal conductivity (k-value). Energy used for space heating and cooling can be decreased by using low-thermal-conductivity materials. The k-value of insulation materials depends on the material's density, porosity, moisture content and temperature. In general, a higher temperature leads to higher k-values at higher material density (Bo-Ming et al. 2008; Budaiwi and Abdou 2013; Budaiwi et al. 2002). The thermal conductivity is also linked to the moisture content inside the material, higher k-values are obtained when the moisture content raises (Budaiwi and Abdou 2013; Kondo et al. 2010). Consequently, the variations of k-value with moisture content of insulation materials must be investigated in order to evaluate their influence on building's energy performance.

This study investigates the manufacturing of novel bio-insulation materials based on bamboo fibers and bone glue, pure or modified by sodium lignosulfonate. The hygrothermal behavior of these materials is investigated by experiments under controlled conditions. In particular, the hygrothermal performance is evaluated through thermal conductivity and isothermal vapor sorption at equilibrium state. Moreover, mechanical properties are assessed through bending measurement.

2 Materials and Experiment

2.1 Materials

Bone glue is a protein-based adhesive made from collagen of bones. It has a granular form and is soluble in water. It was supplied by Briançon Inc., France.

Sodium lignosulfonate is used in the food industry as a de-foaming agent for paper production and in adhesives for items that come in contact with food. It was purchased from Carl Roth GmbH$^+$ Co. KG Inc., Karlsruhe, Germany. It is in powder form and its miscibility with water at 20 °C is 600 g/l. Its melting point is higher than 130 °C and it has a bulk density at 20 °C of 500 kg/m^3.

Bamboo fibers (bambusa stenostachya) were collected at scientific research center for conservation of natural resources, Vietnam. The fibers were extracted from bamboo trees by roller mill technique (RMT) (Deshpand et al. 2000). Then, the fibers were more finely separated by using a specific machine at high speed (29,000 rpm) for one min.

2.2 Preparation of Bamboo Fiberboards

The fiberboards were prepared by pressed method on a hydraulic press. The glues solutions were prepared by swelling 30 g of glues in 200 g of water until completely dissolved. The bamboo fibers and glue solutions were manual mixed and kept in oven at 100 °C for 24 h in order to remove water. Once dried, the mixture was poured into an aluminum mold which has been covered by an adhesive anti-stick coated. The press conditions set up at 150 kgf/cm^2, 160 °C and 15 min. The fiberboards were removed

Table 1. Bamboo fiberboards components

Components			
Samples	Bamboo fibers %(w/w)*	Bone glue %(w/w)	Sodium lignosulfonate %(w/w)
F100	100	0	0
FB9010	90	10	0
FB7030	70	30	0
FBS70273	70	27	3
FBS70219	70	21	9
FS7030	70	0	30

*w/w: weight ratio

from the mold after cooling to room temperature at least 24 h to avoid warping phenomena. The composition of materials is listed in Table 1. The specimens of each material are prepared for further characteristics tests.

2.3 Density Fiberboards Measurement

The density of fiberboards was determined according to EN 323 standard. The specimens were cut and pre-conditioned at 57%RH and 25 °C before being tested. At least five specimens of each material were tested. The density value (kg/m^3) was calculated with the formula below:

$$\rho = W/(a \times b \times c)$$

where: a, b, c (m) and W (kg) is the length, width, thickness and weight of specimen respectively.

2.4 Hygrothermal Characterization Tests

2.4.1 Test Facility

In this study, all hygrothermal properties of insulation materials were measured using closed climatic chamber (called "RH-Box") (Fig. 1) which is made by two chambers connected by an airlock. Temperature and relative humidity in the RH-Box are controlled by heat exchangers and saturated salt solutions. Two fans inside the RH-Box homogenize the atmosphere when the humidity level is changed, but they are stopped when the experiments are in progress. The mass change of specimens during testing can be measured directly in the chamber through a holder that is connected with a microbalance located on the top of the chamber. The temperature and the relative humidity inside the RH-box are recorded with hygrothermal sensors.

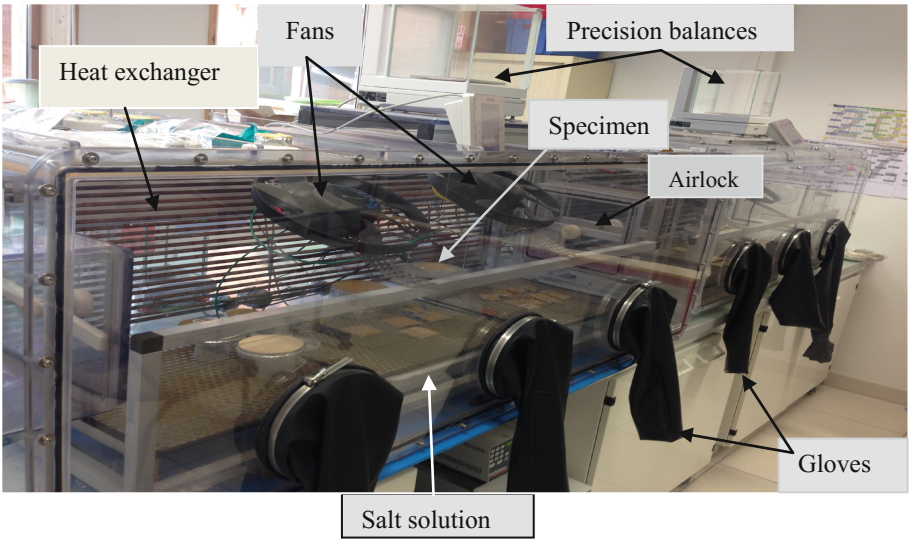

Fig. 1. Climatic chamber (RH-Box)

2.4.2 Water Vapor Sorption Kinetics Until Equilibrium

The kinetic of water vapor sorption isotherm of the fiberboards were examined at three successive relative humidity steps: 33% with $MgCl_2$ solution, 75% with NaCl solution and 33% again. In addition, before being tested, all the specimens were pre-conditioned at 9% RH with a KOH solution at 25 °C. During the period test, the specimen weight evolution is recorded by a precision balance (±0.2 mg), connected to an automatic recording system until reaching at equilibrium state. The temperature during this experiment was kept constant at 25 °C. The water vapor sorption kinetics at equilibrium curves of the specimens were obtained by plotting weight gain/loss percentages function of time.

2.5 Porous Structure of Materials

In this study, porosity degree, average pores diameter, specific surface area and pore size distribution of fiberboards were determined by mercury intrusion porosimetry. In general, the MIP method is based on the non-wetting liquid will only intrude capillaries under pressure, the mercury is slowly intruded into the pores of the materials (ISO15901-1). Before being tested, the samples are air-dried for 24 h; the dried specimens are cut into small pieces and placed in glass vessels. The pores structure parameters are performed by a mercury porosimetry technique (Micromeritics AutoPore IV 9520) under a pressure up to 400 MPa. The MIP method can detect the pores with the radius ranging from 7 nm up to 400 μm. The pore size distribution is identified from the volume of mercury intruded at each pressure increment, while the total porosity is based on the total intruded volume. The equivalent pore radii (r) is calculated based on the known intrusion pressure of mercury (p_{Hg}):

$$r = -\frac{2\gamma_{Hg}.\cos\theta_{Hg}}{p_{Hg}}$$

where: the surface tension of mercury $\left(\gamma_{Hg}\right)$ is assumed as 0.48 N/m and the contact angle of mercury on the hardened mortar surface $\left(\theta_{Hg}\right)$.

2.6 Thermal Conductivity Measurement

The thermal conductivity of fiberboards was measured at 25 °C according to the EN 12664 standard with a TCi-Therm device using the modified transient plane source (MPTS) technique. The test specimens were cut into squares measuring 50 ± 1 mm and pre-conditioned at 57% RH and 25 °C until reaching a constant mass before being tested. Thermal conductivity was then measured inside the RH-Box at different relative humidity levels. This enables to measure the variation of thermal conductivity according to the variation of the moisture content of the specimens. The relationship between the thermal conductivity and the density, the relative humidity and the moisture content was investigated.

2.7 Mechanical Properties

The bending properties including the bending strength and elastic modulus were evaluated according to the EN 310 standard. The test specimens were cut to 150 mm × 25 mm × 6 mm. Before being tested, all the specimens were preconditioned at 57% RH and 25 °C until reaching a constant mass. The average values of the elastic modulus and bending strength at break were calculated based on at least five measurements.

3 Results and Discussion

3.1 Characteristics of Bamboo Fibers

The various components and distribution of the length and diameter of bamboo fibers in this study are shown in Fig. 2. The results indicate that the length distribution ranges from 0 to 7.0 cm and is mainly concentrated at approximately 1.0–2.0 cm, whereas the diameter ranges from 0.16 to 0.52 mm and is mainly concentrated between 0.24 and 0.40 mm. It can be observed that the bamboo fibers have a narrow distribution of diameter and length. Indeed, the preparation of bamboo fibers using rollers is a suitable method to extract a large amount of fibers of quite homogeneous length and small diameter. In addition, this kind of bamboo contains the same amount of components as other different bamboo fibers, but they differ from the components of other natural fibers (Hill et al. 2009).

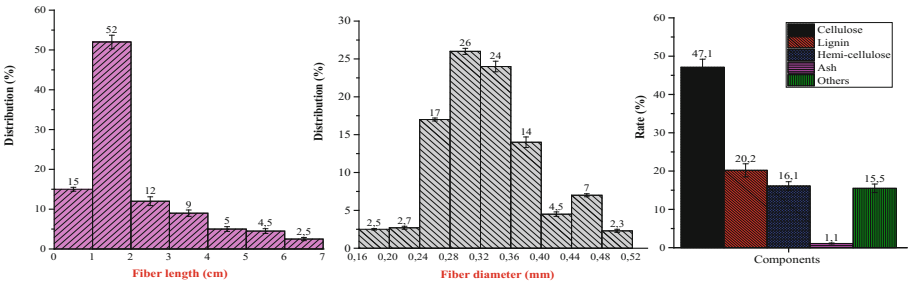

Fig. 2. Length, diameter distribution and components of bamboo fibers (Nguyen et al. 2017).

3.2 Mercury Intrusion Porosimeter (MIP)

Microstructure of the three highlighted fiberboards was examined by mercury intrusion porosimeter method. Their porosity, average pore diameter, pore volume and pore size distribution were illustrated in Fig. 3 and Table 2. The MIP result shows a higher porosity at 76% for the fiberboard without glue (F100), 64% porosity for FB7030, which used 30% bone glue and 49% porosity for FBS70219 using 30% mixture glue between bone and sodium lignosulfonate. In addition, the pore size distribution of three fiberboards is largely ranged from 0.005 to 100 μm and it was classified to three

categories: capillary pores (0.005–0.1 μm), mesopores (0.1–10 μm) and air pores (>10 μm) as previous literature (Penttala 1989; Wang et al. 2017). This result could be contributed by the level of compaction, the effective adhesion of glues which verified through mechanical properties of these boards as Fig. 8 (Wang et al. 2016). In particular, the effective of binders influenced on the average pores diameter of fiberboards, which represents 82 nm for FBS70219 and 219 nm for FB7030 while the F100 exhibited the largest average pores diameter of 1,135 nm, which consist of more voids between the fibers, leading to more incremental pore volume and porosity (Choi et al. 2009; Westermarck et al. 1998). Conversely, the F100 has a lowest total pore area at 7.4 (m^2/g) in comparison to FB7030 (23.5 m^2/g) and FBS70219 (27.7 m^2/g) respectively. The results can be explained by the large pores and densely distributed pores can result in a much smaller total surface area in the same volume. Indeed, the small pores have a significant influence on the total surface area and interface of fiberboards (Choi et al. 2009). Additionally, the higher specific pore surface leads to higher hygroscopic capacity of boards.

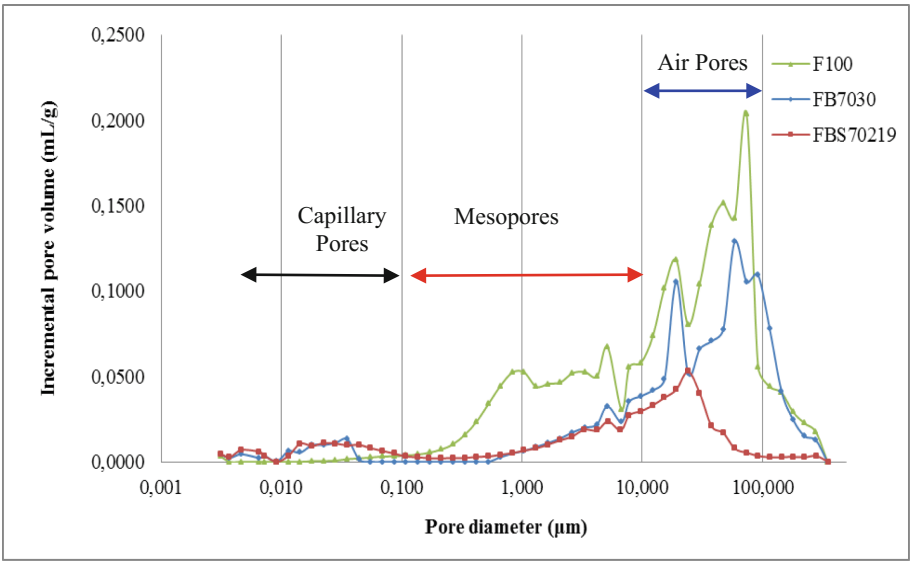

Fig. 3. Microstructure properties of three highlighted boards: pore volume function with pore diameter distribution

Table 2. The porous structure parameters of bamboo boards obtained by MIP

Material	Porosity (%)	Average pore diameter (nm)	Specific total pore area (m^2/g)
F100	76.1	1,135	7.4
FB7030	64.6	219	23.5
FBS70219	49.7	82	27.7

3.3 Kinetics of Water Vapor Sorption

The vapor sorption kinetics of the bamboo fiberboards were examined under temperature and relative humidity protocol described in scheme Fig. 4a. The amount of moisture absorbed, and residual moisture as well as moisture sorption behavior of the fiberboards at three equilibriums at 33-75-33% RH are observed in Fig. 4b.

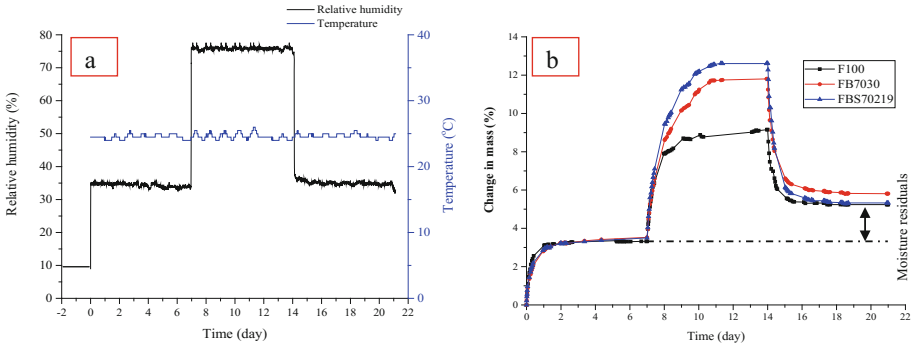

Fig. 4. Kinetics of water vapor sorption at equilibrium state: (a) humidity and temperature protocol (9-33-75-33% RH) at 25 °C, (b) kinetics curves and moisture sorption capacity

The first equilibrium was reached at 33%RH after pre-conditioning at 9%RH. The three fiberboards absorbed the same amount of moisture (about 3.5%) after less than two days with a similar shape of absorption curves. During the equilibrium at 33%RH, that the water molecules are absorbed as monolayer on the pores surfaces (Latif et al. 2014). This phenomenon leads to the same amount of moisture uptake capacity of three boards.

The second equilibrium was reached at 75%RH. The F100 exhibited an amount of moisture uptake about 9.5% after reaching equilibrium, which is lower than for FB7030 and FBS70219 with around 11.8% and 12.6% respectively. The board F100 reaches the second equilibrium after 3 days while FB7030 and FBS70219 required 4 days. The time required to reach equilibrium of these fiberboards associated to their moisture absorption capacity (Ge et al. 2014). At equilibrium (75%RH), the FBS70219 has a higher moisture uptake value (12.6%) compared to the FB7030 (11.8%) and F100 (9.5%). The different amount of equilibrium moisture absorption is due to the higher moisture absorption capacity of sodium lignosulfonate and protein based on bone glues compared to bamboo fibers.

Additionally, during the equilibrium, between 33% and 75% RH, the water molecules are absorbed as multilayers and condensation can occur in pores and capillaries (Latif et al. 2014). Thus the higher amount of moisture absorbed by the boards FBS70219 and FB7030 is also due to their pore volume in capillary zone (Fig. 3), as well as their average pore diameter compares to F100.

During the RH decrease to the last equilibrium at 33%, the moisture desorption of the fiberboards appeared rapidly and equilibrium is reached after only one day exposure to 33%RH. However, the amount of moisture uptake in absorption process (from 33% to 75%RH) is not totally discharged in desorption process and doesn't return to the level reached during the first exposure at 33%RH. Consequently, a significant amount of residual moisture remains in the three fiberboards. The Fig. 4b exhibits an amount of residual moisture about 2.3% for FB7030, 1.9% for F100 and 1.8% for FBS70219 compared to the first equilibrium at 33%RH. The residual moisture phenomenon of fiberboards was explained via the capillary condensation hysteresis and the moisture trapped inside large pores with small necks (ink-bottle effect) (Collet et al. 2008).

3.4 Thermal Conductivity of the Fiberboards

3.4.1 Influence of Density

Figure 5 shows the thermal conductivity as function of the density at 57%RH and 25 °C. The result indicates that the FBS70219 board has a highest density about 538 ± 12 kg/m^3, associating with the highest thermal conductivity of approximately 0.088 W m^{-1}K^{-1}. The two FS7030 and FB9010 boards with a low-range density, about 311 ± 22 and 320 ± 24 kg/m^3 respectively, correspond to low thermal conductivity values around 0.055 and 0.057 W m^{-1}K^{-1}. The three other boards (F100, FB7030 and FB70273) have intermediate densities (431 ± 15, 382 ± 18 and 442 ± 18 kg/m^3 respectively) with a similar range of thermal conductivity values: 0.077, 0.082 and 0.081 W m^{-1}K^{-1} respectively. The different thermal conductivity is due to the different density of bamboo fiberboards. The influence of bone, sodium lignosulfonate and

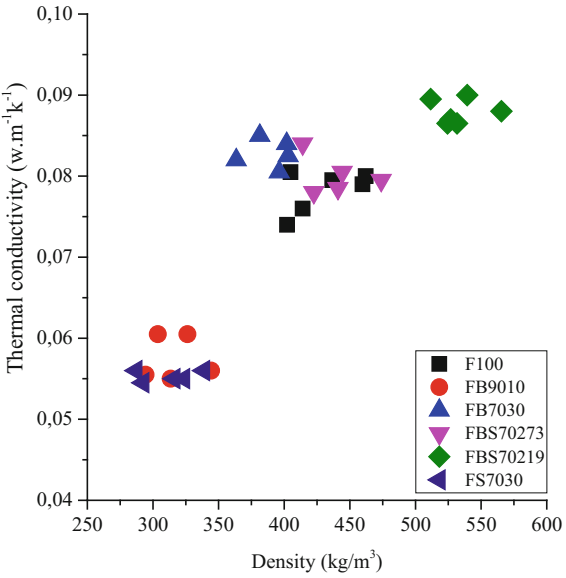

Fig. 5. Thermal conductivity versus density of fiberboards at 57%RH, 25 °C (Nguyen et al. 2017)

fibers/glue ratio induced the different compaction levels of the boards (Ratiarisoa et al. 2016). Low-density boards with the lack of glues contain more voids and thus more air. Thermal conductivity of air being lower than that of solid materials, the presence of voids in the boards results in a lower thermal conductivity for the low-density boards (Abdou and Budaiwi 2013; Sjöström and Blomqvist 2014; Suleiman et al. 1999).

Compared to other published literature, the thermal conductivity of bamboo fiberboards is lower than that of corn cob board (Verdier and Granulats 2012), cotton stalk fiberboard (Zhou et al. 2010), durian peel/coconut coir board (Khedari and Teekasap 2004) and wood (pine) board (Xu et al. 2004). It can be observed that the thermal conductivity of bamboo fiberboards is in the low range for such insulating building materials.

3.4.2 Influence of Moisture

Figure 6 shows the influence of relative humidity levels on thermal conductivity at 25 °C. Thermal conductivity was measured when the specimens reached equilibrium state at 33% and 75%RH. It can be observed that at a relative humidity level of 75%, the thermal conductivity of these boards was increased and it was decreased when specimens were exposed to a lower relative humidity (33%RH). The increase of thermal conductivity at 75%RH is due to the rise of moisture amount in the specimens. The reverse behavior (decrease) was observed when the specimens were moved from 75%RH to 33%RH because the moisture evaporated leading to more voids in the fiberboards (Abdou and Budaiwi 2013; Shiva et al. 2014; Sjöström and Blomqvist 2014; Suleiman et al. 1999). Additionally, the thermal conductivity variations according to relative humidity levels (33% and 75%RH) are indicated in Table 3.

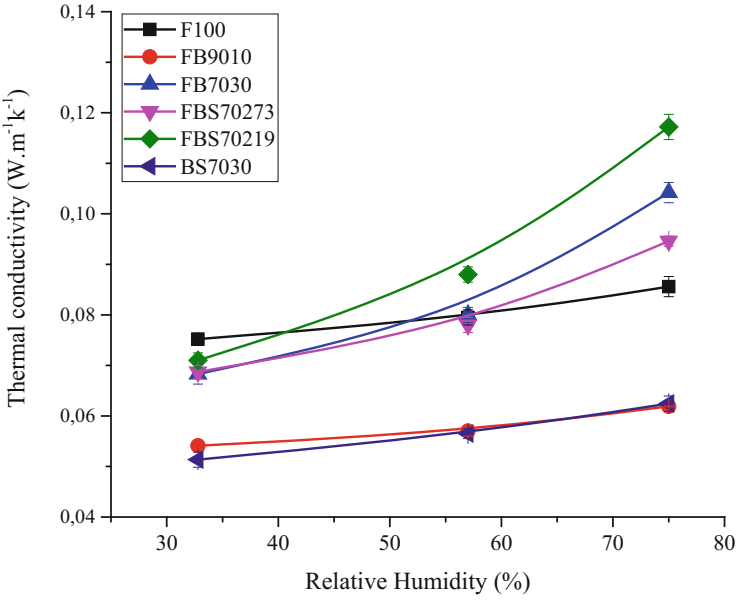

Fig. 6. Variation of thermal conductivity with relative humidity at 33% and 75%RH at 25 °C

Table 3. Variation of the thermal conductivity (Δk-value) with moisture uptake/release (ΔMC) of fiberboards at 33 and 75% relative humidity (Nguyen et al. 2017).

Samples	Density (kg/m^3)	ΔMC uptake at 75%RH (%)	ΔMC release at 33%RH (%)	(Δk-value) increase at 75%RH (%)	(Δk-value) decrease at 33%RH (%)
F100	431 ± 25	3.2 ± 0.4	0.4 ± 0.1	11.6 ± 2.4	3.5 ± 1.0
FB9010	320 ± 24	4.6 ± 0.6	1.4 ± 0.3	7.5 ± 1.5	8.9 ± 1.2
FB7030	382 ± 18	7.0 ± 0.7	2.9 ± 0.6	26.8 ± 3.2	16.7 ± 1.6
FBS70273	442 ± 28	7.7 ± 0.6	2.8 ± 0.2	16.8 ± 3.0	15.2 ± 1.4
FBS70219	538 ± 27	9.0 ± 0.8	2.7 ± 0.3	34.2 ± 3.4	19.2 ± 1.8
FS7030	311 ± 22	5.8 ± 1.1	3.6 ± 0.7	12.8 ± 2.2	7.1 ± 1.6

Additionally, a linear regression was observed for relationship between thermal conductivity and relative humidity for each sample (Fig. 6). However, the slopes are different due to the different materials' vapor sorption capacity (Table 3). In fact, the thermal conductivity evolves linearly until the value corresponding to the equilibrium moisture level. It can be thought that the moisture penetrates quickly all the sample volume from the beginning of the moisture exposition instead of accumulating in the surface region before migrating to the inner layers. This result match with some materials in previous literature such as: wood fiber, oriented strand board, and narrow-ring wood (Abdou and Budaiwi 2013; Vololonirin et al. 2014).

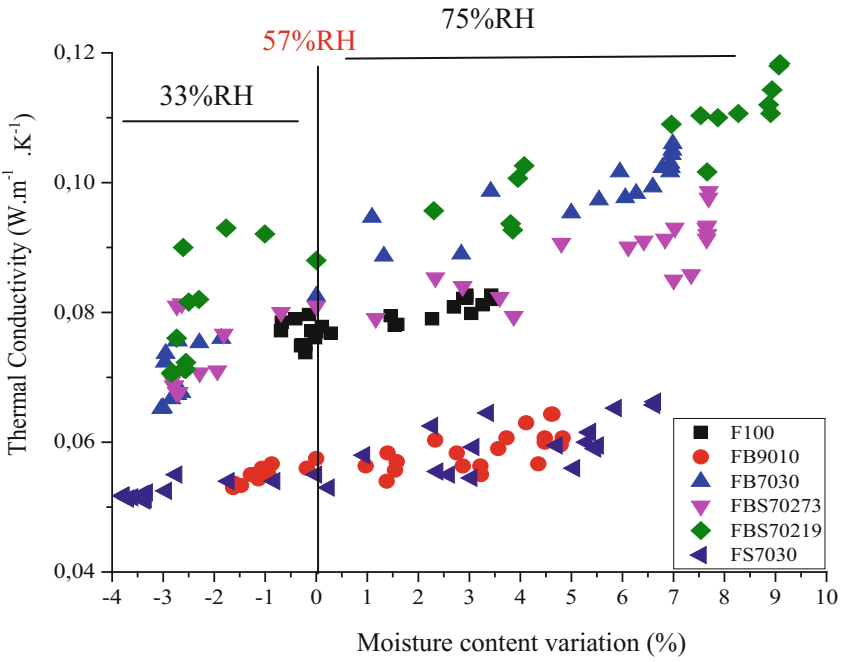

Fig. 7. Evolution of thermal conductivity with moisture content variations for the fiberboards at 25 °C between 33% and 75%RH

Moreover, the thermal conductivity was measured all along the moisture uptake from 33% RH to 75% RH. The variation moisture content (ΔMC) was calculated from weight increment or decrement and weight at pre-conditioned at 57%RH. The relationship between thermal conductivity and moisture content variations of all fiberboards is shown in Fig. 7.

3.5 Bending Properties

The elastic modulus and bending strength of all bamboo fiberboards are shown in Fig. 8. The elastic modulus and the bending strength reach 3131 MPa and 7.3 MPa for 30% (w/w) bone glue (FB7030) compared to the board without glue (F100) (elastic modulus of 1310 MPa and bending strength of 2.7 MPa). In fact, bone glue acts as an internal binder and ensures the cohesion inside the fiberboards (Evon et al. 2010). However, 10% (w/w) bone glue is not sufficient to ensure a good adhesion between the fibers, whereas 30% (w/w) bone glue provides better adhesion at the interfaces between the bone glue and bamboo fibers.

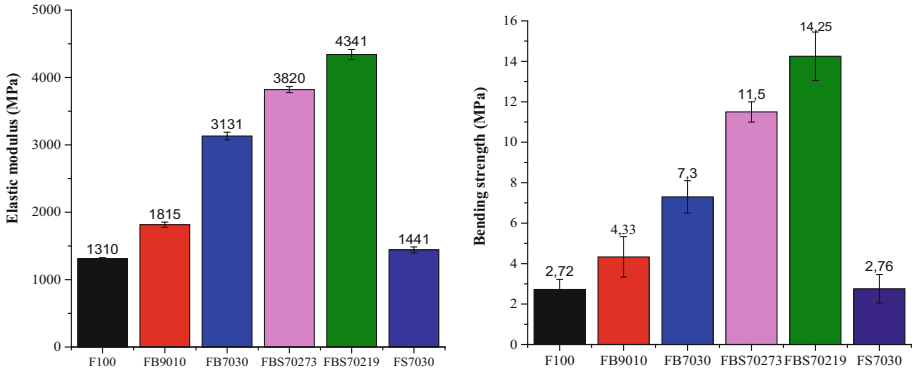

Fig. 8. Bending properties of fiberboards at 57% RH and 25 °C (Nguyen et al. 2017)

On the other hand, the bending properties of the fiberboards are strongly affected by the addition of sodium lignosulfonate. Adding sodium lignosulfonate to bone glue improves the elastic modulus and bending strength of fiberboards. The FBS70219 boards with 9% (w/w) of sodium lignosulfonate presented an increase of elastic modulus of approximately 4341 MPa and a bending strength about 14.3 MPa. This result can be explained that the sodium lignosulfonate is stiffer than protein, high molecular weight and the large quantity of aromatic rings of sodium lignosulfonate provide a stiffer material and improve its mechanical properties (Baumberger et al. 1998). A cross-linked network is formed between protein molecules of bone glue and sodium lignosulfonate leading to strong interactions in the boards as covalent bonds and also hydrogen and hydrophobic interactions (Frihart and Birkeland 2014; Huang and Chen 2003).

4 Conclusion

Six different types of bio-insulation materials have been manufactured from bamboo fibers and different bio-glues by thermo-pressing. The optimum fiberboard mechanical properties are obtained with a ratio of 70% (w/w) bamboo fibers and 30% (w/w) mixture glue of bone and sodium lignosulfonate (FBS70219, E = 4341 MPa and σ_r = 14 MPa). The thermal conductivity of fiberboards from bamboo fibers and different glue ratios is fairly low, varying between 0.057 and 0.088 W $m^{-1}K^{-1}$ at 25 °C and 57%RH. Variation of thermal conductivity k with relative humidity and moisture content plays an important role in evaluating the hygrothermal performance of materials. As expected, k increases with moisture content variations of the samples. For all the fiberboards with 30% of glue this increase is proportionally nearly the same. It can be concluded that the bamboo fiberboards and more specially the FBS70219 panel are promising materials to participate in buildings' moisture control and is saving energy.

Acknowledgements. The authors would like to thank the Eiffel Excellence Scholarship Programme, Région Rhône-Alpes and Agence Nationale de la Recherche (ANR) for financial support. This work was also supported by a grant from Vietnam National University Ho Chi Minh City (VNU-HCM) project number HS2014-48-01. We thank all the participants for their enthusiasm, discussions and cooperation in this study.

References

Abdou, A., Budaiwi, I.: The variation of thermal conductivity of fibrous insulation materials under different levels of moisture content. Constr. Build. Mater. **43**, 533–544 (2013)

Baumberger, S., Lapierre, C., Monties, B.: Utilization of pine kraft lignin in starch composites: impact of structural heterogeneity. J. Agric. Food Chem. **46**, 2234–2240 (1998)

Bo-Ming, Z., Zhao, S., He, H.: Experimental and theoretical studies of hightemperature thermal properties of fibrous insulation. J. Quant. Spectrosc. Radiat. Transf. **109**, 1309–1324 (2008)

Budaiwi, I., Abdou, A.: The impact of thermal conductivity change of moist fibrous insulation on energy performance of buildings under hot-humid conditions. Energy Build. **60**, 388–399 (2013)

Budaiwi, I., Abdou, A., Homoud, M.A.: Variation of thermal conductivity of insulation materials under different operating temperatures: impact on envelope-induced cooling load. J. Archit. Eng. **8**, 125–132 (2002)

Choi, H.Y., Han, S.O., Lee, J.S.: The effects of surface and pore characteristics of natural fiber on interfacial adhesion of henequen fiber/PP biocomposites. Compos. Interfaces **16**, 359–376 (2009)

Collet, F., Bart, M., Serres, L., Miriel, J.: Porous structure and water vapour sorption of hemp-based materials. Constr. Build. Mater. **22**, 1271–1280 (2008)

Cong, F., Diehl, B.G., Hill, J.L., Brown, N.R., Tien, M.: Covalent bond formation between amino acids and lignin: cross -coupling between proteins and lignin. Phytochemistry **96**, 449–456 (2013)

Deshpand, A.P., Bhaskar, R.M., Lakshmana, R.C.: Extraction of bamboo fibers and their use as reinforcement in polymeric composites. J. Appl. Polym. Sci. **76**, 83–92 (2000)

Duval, A., Molina-Boisseau, S., Chirat, C.: Comparison of kraft lignin and lignosulfonates addition to wheatgluten-based materials: Mechanical and thermal properties. Ind. Crops Prod. **49**, 66–74 (2013)

Evon, P., Vandenbossche, V., Pontalier, P.Y., Rigal, L.: Thermo-mechanical behaviour of the raffinate resulting from the aqueous extraction of sunflower whole plant in twin-screw extruder: manufacturing of biodegradable agromaterials by thermo-pressing. Adv. Mater. Res. **112**, 67–72 (2010)

Frihart, C.R., Birkeland, M.J.: Soya Properties and Soy Wood Adhesives. American Chemical Society, Washington, D.C. (2014)

Ge, H., Yang, X., Fazio, P., Rao, J.: Influence of moisture load profiles on moisture buffering potential and moisture residuals of three groups of hygroscopic materials. Build. Environ. **81**, 162–171 (2014)

Hauptmann, M., Lubin, J.H., Stewart, P.A., Hayes, R.B., Blair, A.: Mortality from solid cancers among workers in formaldehyde industries. Am. J. Epidemiol. **159**, 1117–1130 (2004)

Hill, C.A.S., Norton, A., Newman, G.: The water vapor sorption behavior of natural fibers. J. Appl. Polym. Sci. **112**, 1524–1537 (2009)

Huang, J., Chen, L.Z.P.: Effects of lignin as a filler on properties of soy protein plastics. II. Alkaline lignin. J. Appl. Polym. Sci. **88**, 3291–3297 (2003)

ISO15901-1: Evaluation of pore size distribution and porosimetry of solid materials by mercury porosimetry and gas adsorption – part 1: mercury porosimetry

Kaewtatip, K., Menut, P., Auvergne, R.: Interactions of kraft lignin and wheat gluten during biomaterial processing: evidence for the role of phenolic groups. J. Agric. Food Chem. **58**, 4185–4192 (2010)

Khedari, J., Teekasap, S.: New low-cost insulation particleboards from mixture of durian peel and coconut coir. Build. Environ. **39**, 59–65 (2004)

Khosravi, S., Nordqvist, P., Khabbaz, F., Johansson, M.: Protein-based adhesives for particleboards—effect of application process. Ind. Crops Prod. **34**, 1509–1515 (2011)

Kondo, Y., Hvamac, A., Nagasa, W.L.Y., Fujimoto, T., Kikuchi, Y., Tasaka, T.: Experiments on influence of moisture on thermal performance change of insulations: Long term thermal performance of building insulation materials Part 2. J. Environ. Eng. **75**, 261–269 (2010)

Kunanopparat, T., Menut, P., Morel, M.H.N., Guilbert, S.: Modification of the wheat gluten network by kraft lignin addition. J. Agric. Food Chem. **57**, 8526–8533 (2009)

Kunanopparat, T., Menut, P.P., Morel, M.H., Guilbert, S.: Improving wheat gluten materials properties by kraft lignin addition. J. Appl. Polym. Sci. **125**, 1391–1399 (2012)

Latif, E., Tucker, S., Ciupala, M.A., Wijeyesekera, D.C., Newport, D.: Hygric properties of hemp bio-insulations with differing compositions. Constr. Build. Mater. **66**, 702–711 (2014)

Michael, H., Patricia, A.S., Jay, H.L.: Mortality from lymphohematopoietic malignancies and brain cancer among embalmers exposed to formaldehyde. J. Natl Cancer Inst. **101**, 1696–1708 (2009)

Nguyen, D.M., Grillet, A.C., Diep, T.M.H., Ha-Thuc, C.N., Woloszyn, M.: Hygrothermal properties of bio-insulation building materials based on bamboo fibers and bio-glues. Constr. Build. Mater. **155**, 852–866 (2017)

Penttala, V.: Effects of microporosity on the compression strength and freezing durability of high-strength concretes. Mag. Concr. Res. **41**, 171–181 (1989)

Ratiarisoa, R.V., Magniont, C., Ginestet, S., Oms, C., Escadeillas, G.: Assessment of distilled lavender stalks as bioaggregate for building materials: hygrothermal properties, mechanical performance and chemical interactions with mineral pozzolanic binder. Constr. Build. Mater. **124**, 801–815 (2016)

Shiva, K.M., Durga, P.B., Basavaraj, M.: Effect of moisture content and temperature on thermal conductivity of Psidium Guajava L. by line heat source method (transient analysis). Int. J. Heat Mass Transf. **78**, 354–359 (2014)

Sjöström, J., Blomqvist, P.: Direct measurements of thermal properties of wood pellets: elevated temperatures, fine fractions and moisture content. Fuel **134**, 460–466 (2014)

Suleiman, B.M., Larfeldt, J., Leckner, B., Gustavsson, M.: Thermal conductivity and diffusivity of wood. Wood Sci. Technol. **33**, 465–473 (1999)

Verdier, T., Granulats, V.D.: Végétaux Dans Un Matériau De Construction À Matrice Minérale. Université Paul Sabatier, Toulouse (2012)

Vololonirin, O., Coutand, M., Perrin, B.: Characterization of hygrothermal properties of wood-based products – impact of moisture content and temperature. Constr. Build. Mater. **63**, 223–233 (2014)

Wang, L., Chen, S.S., Tsang, D.C.W., Poon, C.S., Dai, J.G.: CO2 curing and fibre reinforcement for green recycling of contaminated wood into high-performance cement-bonded particleboards. J. CO2 Util. **18**, 107–116 (2017)

Wang, L., Chen, S.S., Tsang, D.C.W., Poon, C.S., Shih, K.: Value-added recycling of construction waste wood into noise and thermal insulating cement-bonded particleboards. Constr. Build. Mater. **125**, 316–325 (2016)

Westermarck, S., Juppo, A.M., Koiranen, K., Yliruusi, J.: Mercury porosimetry of pharmaceutical powders and granules. J. Porous Mater. **5**, 77–86 (1998)

Xu, J.Y., Sugawara, R., Widyorini, R., Han, G., Kawai, S.: Manufacture and properties of low-density binderless particleboard from kenaf core. J. Wood Sci. **50**, 62–67 (2004)

Zhigang, X., Yonghui, L., Xiaorong, W., Guangyan, Q., Ningbo, L., Zhang, K., Donghai, W.D., Xiuzhi, S.S.: Utilization of sorghum lignin to improve adhesion strength of soy protein adhesives on wood veneer. Ind. Crops Prod. **50**, 501–509 (2013)

Zhou, X.Y., Zheng, F., Li, H.G., Lu, C.L.: An environment-friendly thermal insulation material from cotton stalk fibers. Energy Build. **42**, 1070–1074 (2010)